The nature, origin, and properties of the one- and two-dimensional optical rogue waves

Stanko N. Nikolić [1,2,*], Sarah B. A. Alwashahi [3], Najdan B. Aleksić [4], Omar A. Ashour [5], Siu A. Chin [6], Milivoj R. Belić [2]

[1] Institute of Physics Belgrade, University of Belgrade, Serbia
[2] Science program, Texas A&M University at Qatar, Doha, Qatar
[3] Faculty of Physics, University of Belgrade, Serbia
[4] Moscow State Technological University "STANKIN", Moscow, Russia
[5] Department of Physics, University of California, Berkeley CA 94720, USA
[6] Department of Physics and Astronomy, Texas A&M University, College Station TX 77843, USA

* E-mail: stankon@ipb.ac.rs

Abstract. The generating mechanism of optical rogue waves (RWs) is the modulation instability (MI). It is the nonlinear optical process in which a weak perturbation of the background pump wave produces an exponential growth of higher order sidebands that constructively interfere to build RWs. We produce RWs in numerical simulations of the cubic nonlinear Schrödinger equation, Hirota, and quintic equation with noisy (or other) inputs on the flat or elliptic background [1,2]. We discuss RWs strange nature, ingrained instability, dynamic generation, and potential applications. We propose the method of mode pruning for suppressing the modulation instability of rogue waves. We further demonstrate how to produce stable Talbot carpets (two dimensional patterns) of rogue waves. We also present statistical analysis [3] on rogue waves produced by various numerical algorithms using white noise as initial conditions.

ENLSE:

$$i\psi_x + S[\psi(x,t)] - i\alpha H[\psi(x,t)] + \gamma P[\psi(x,t)] - i\delta Q[\psi(x,t)] = 0$$

Variables: x – evolutional, t – transversal. Real params: α, γ, δ.

$$S[\psi(x,t)] = \frac{1}{2}\psi_{tt} + |\psi|^2\psi \qquad H[\psi(x,t)] = \psi_{ttt} + 6|\psi|^2\psi_t$$

$$P[\psi(x,t)] = \psi_{tttt} + 8|\psi|^2\psi_{tt} + 6|\psi|^4\psi + 4|\psi_t|^2\psi + 6\psi_t^{\,2}\psi^* + 2\psi^2\psi_{tt}^*$$

$$Q[\psi(x,t)] = \psi_{ttttt} + 10|\psi|^2\psi_{ttt} + 30|\psi|^4\psi_t + 10\psi\psi_t\psi_{tt}^* + 10\psi\psi_t^*\psi_{tt} + 20\psi^*\psi_t\psi_{tt} + 10\psi_t^2\psi_t^*$$

I. Solutions on the uniform background

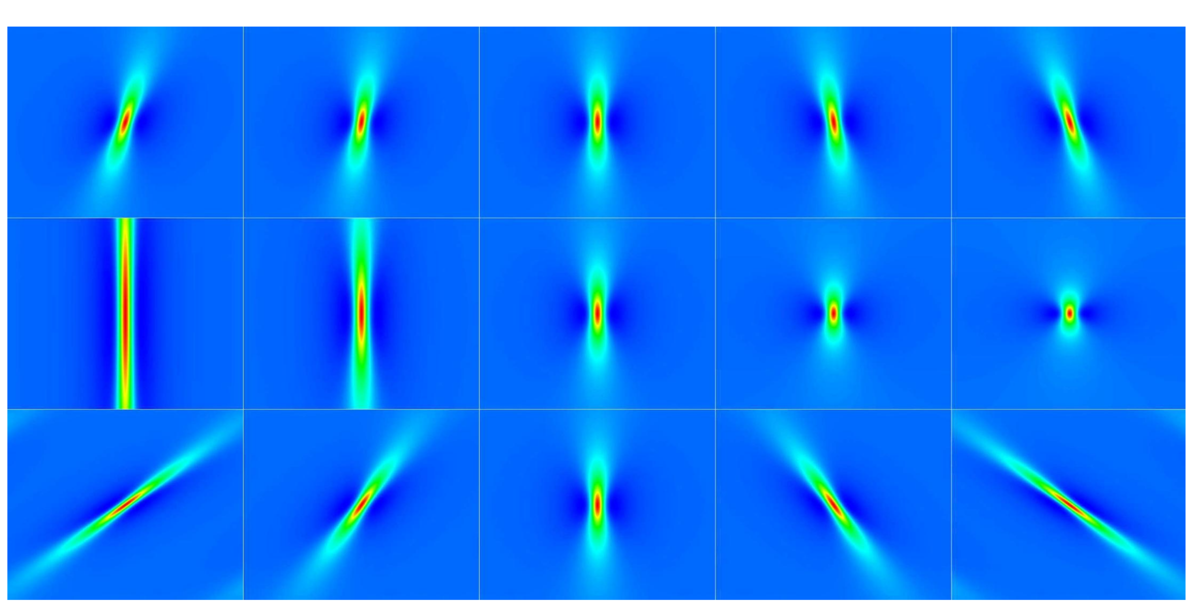

Figure 1: Intensity distribution of the first-order breather. Top row: α spans from -0.1 to 0.1, γ=0, δ=0. Middle row: γ spans from -0.1 to 0.1, α=0, δ=0. Bottom row: δ spans from -0.1 to 0.1, α=0, γ=0

Breather solutions are periodic along *t*-axis with frequency: $\omega = 2\sqrt{1-\nu^2}$

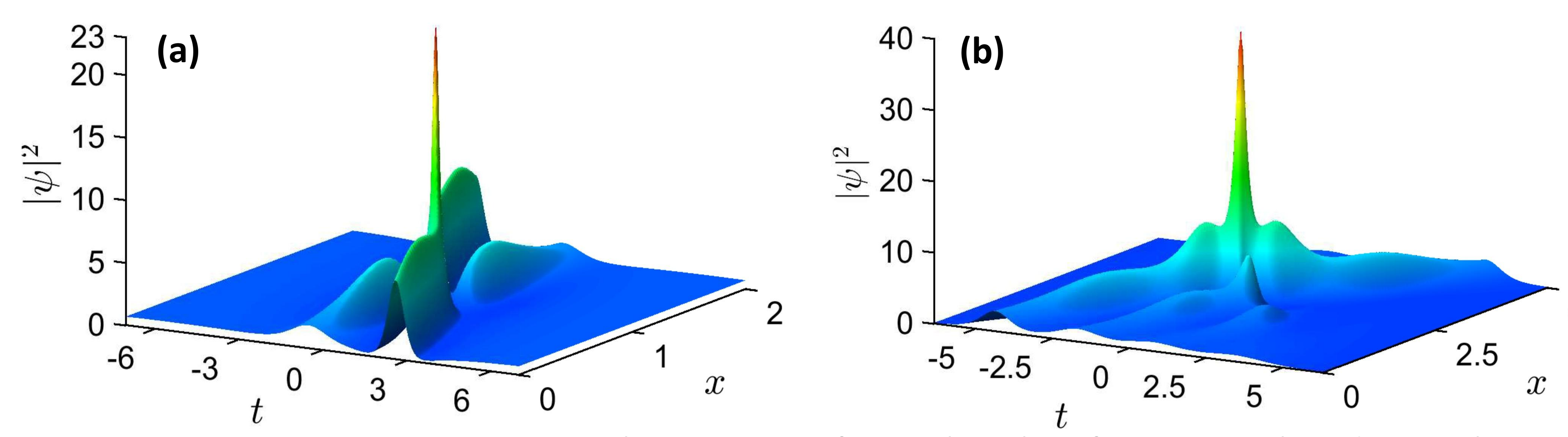

Figure 2: Dynamical propagation of ENLSE breathers from DT initial conditions. The (a) second-order breather with ν_1=0.975, α=0.0625, γ=0.053, δ=0.043, (b) fourth-order breather with ν_1=0.969, α=-0.1625, γ=0.017, δ=0.006

II. Solutions on the nonuniform background

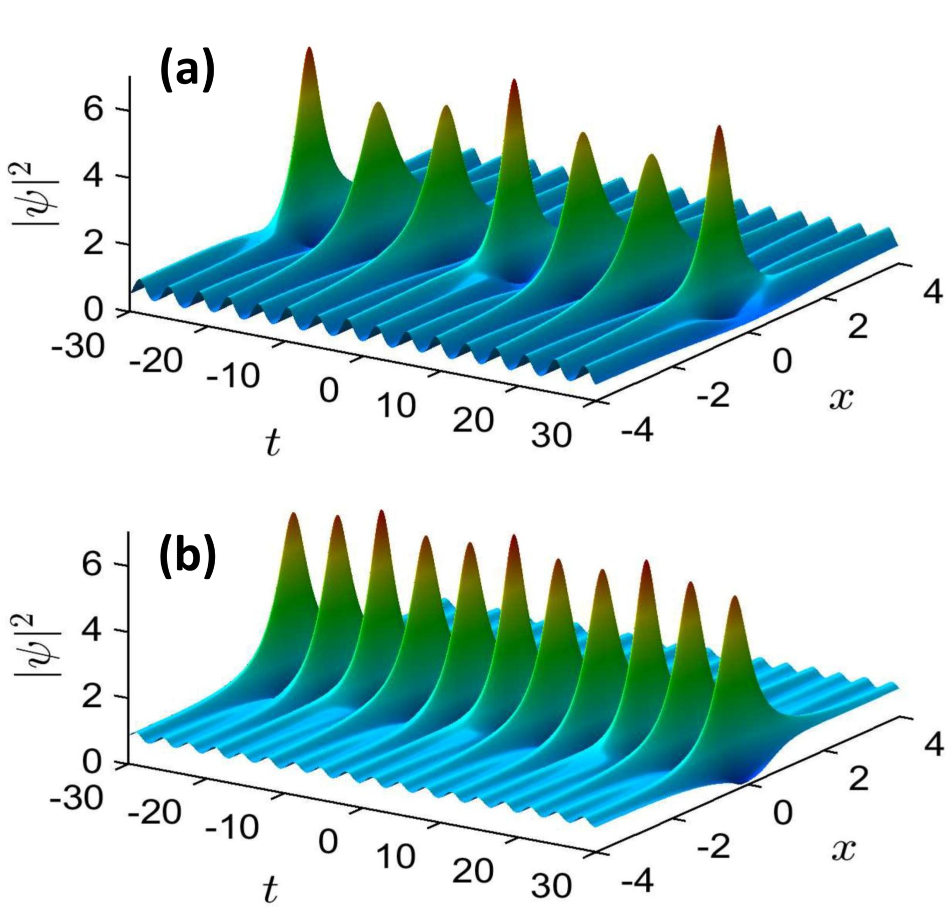

The period of the background *dn* elliptic waves:

$$T_{\mathrm{dn}} = 2\int_0^{\pi/2} \frac{\mathrm{d}\theta}{\sqrt{1-m\sin^2\theta}}$$

Figure 3: First-order breathers on the *dn* background with ν=0.75, α=0.13, γ=0.1, δ=-0.07: (a) $m=0.75^2$, (b) $m=0.5^2$. The breather period also depends on the background parameter *m*

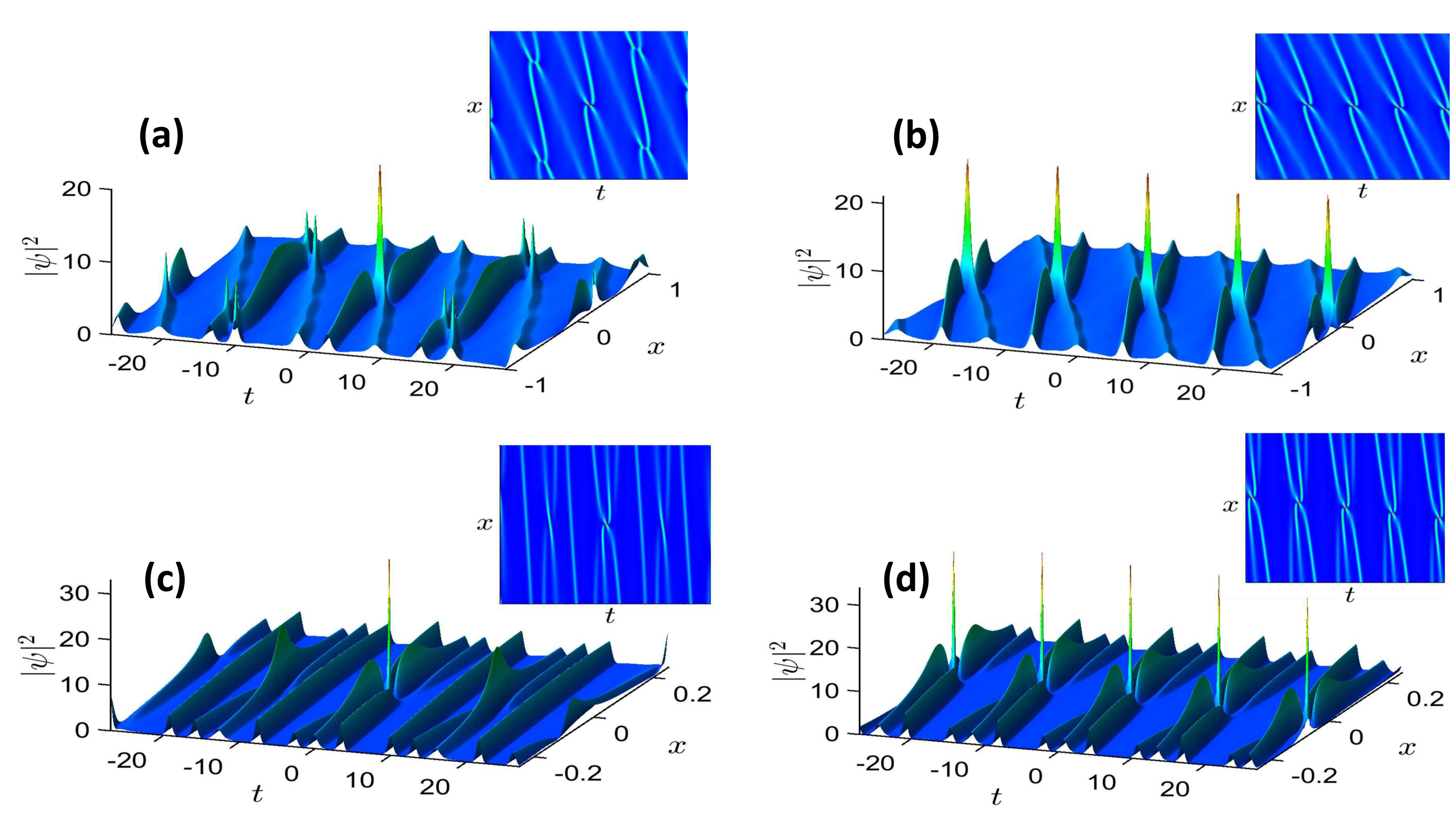

What happens when we match the periods of breather T_B and background T_{dn} ($q = T_B / T_{dn}$)?

Figure 4: 2nd-order breather : (a) Unmatched case, q=3.17, yields single RW, (b) matched case, q=4, produces periodic RWs! The 3rd-order breather : (c) unmatched q=3.17, (d) matched q=4

III. Double-periodic solutions and Talbot carpets

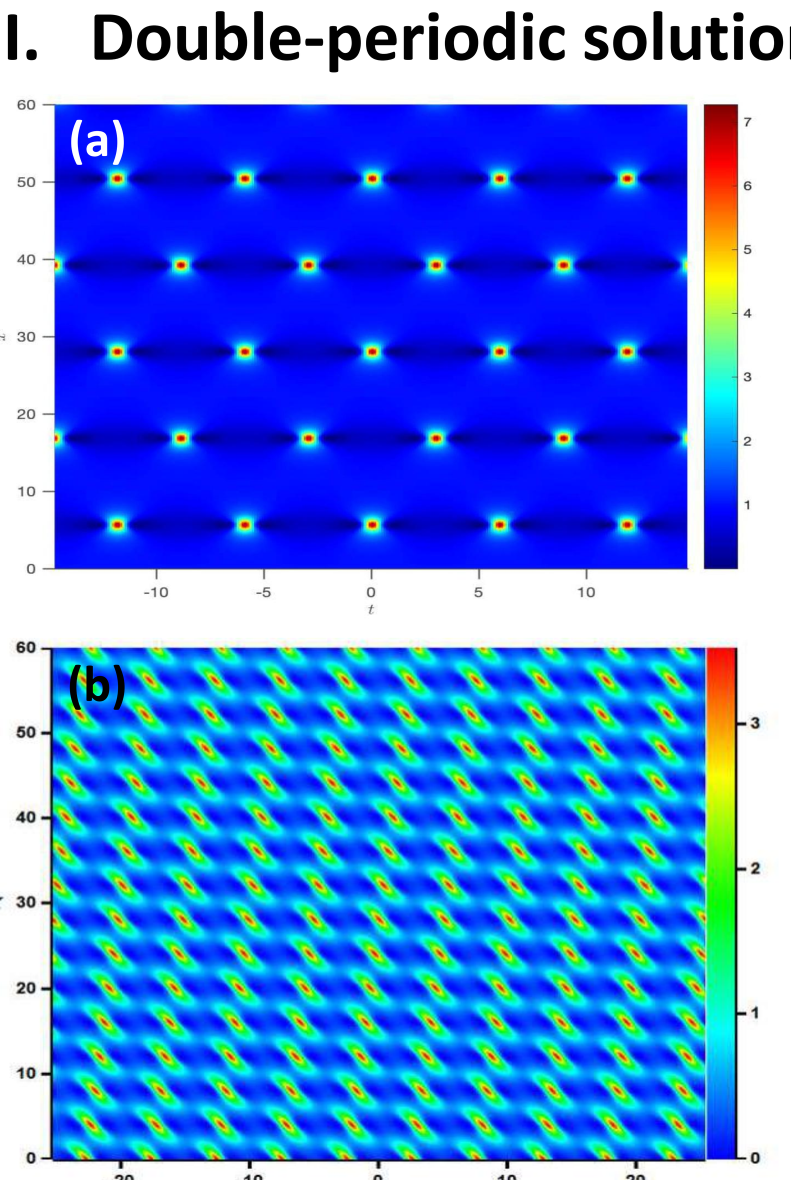

The pruning procedure is used to suppress the growth of unwanted Fourier modes during breather evolution.

Figure 5: (a) Talbot carpet of NLSE (α=γ=δ=0), (b) Evolution of Hirota equation (α=0.2712, γ=δ=0) with modes pruning turned ON

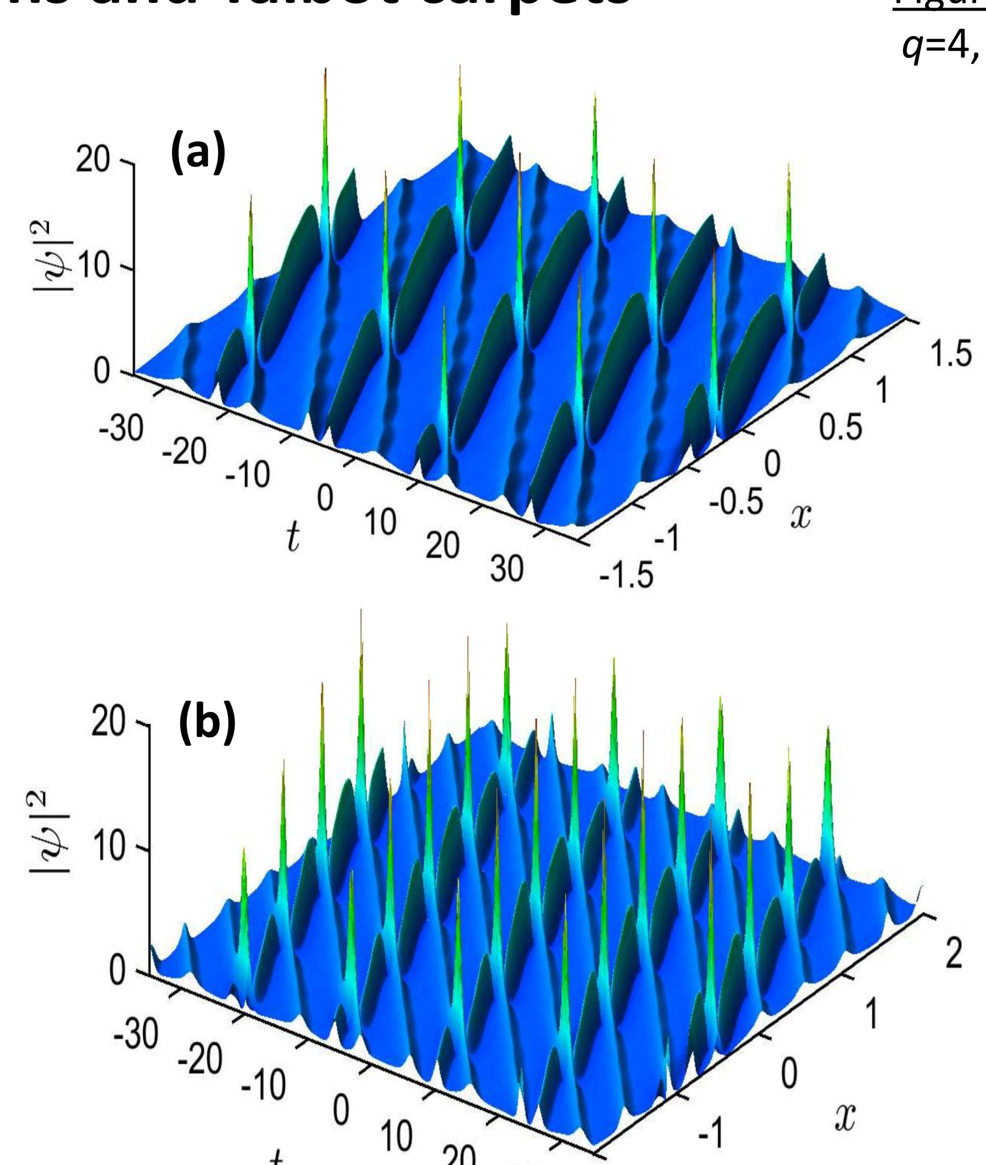

Figure 6: Components of the 2nd-order breather are matched mutually and to the elliptic background wave with α=-0.03, γ=-0.0614, δ=0.7
(a) m=0.1192, ν_1=0.92, ν_2=0.83, q=9,
(b) m=0.0505, ν_1=0.92, ν_2=0.8104, q=8

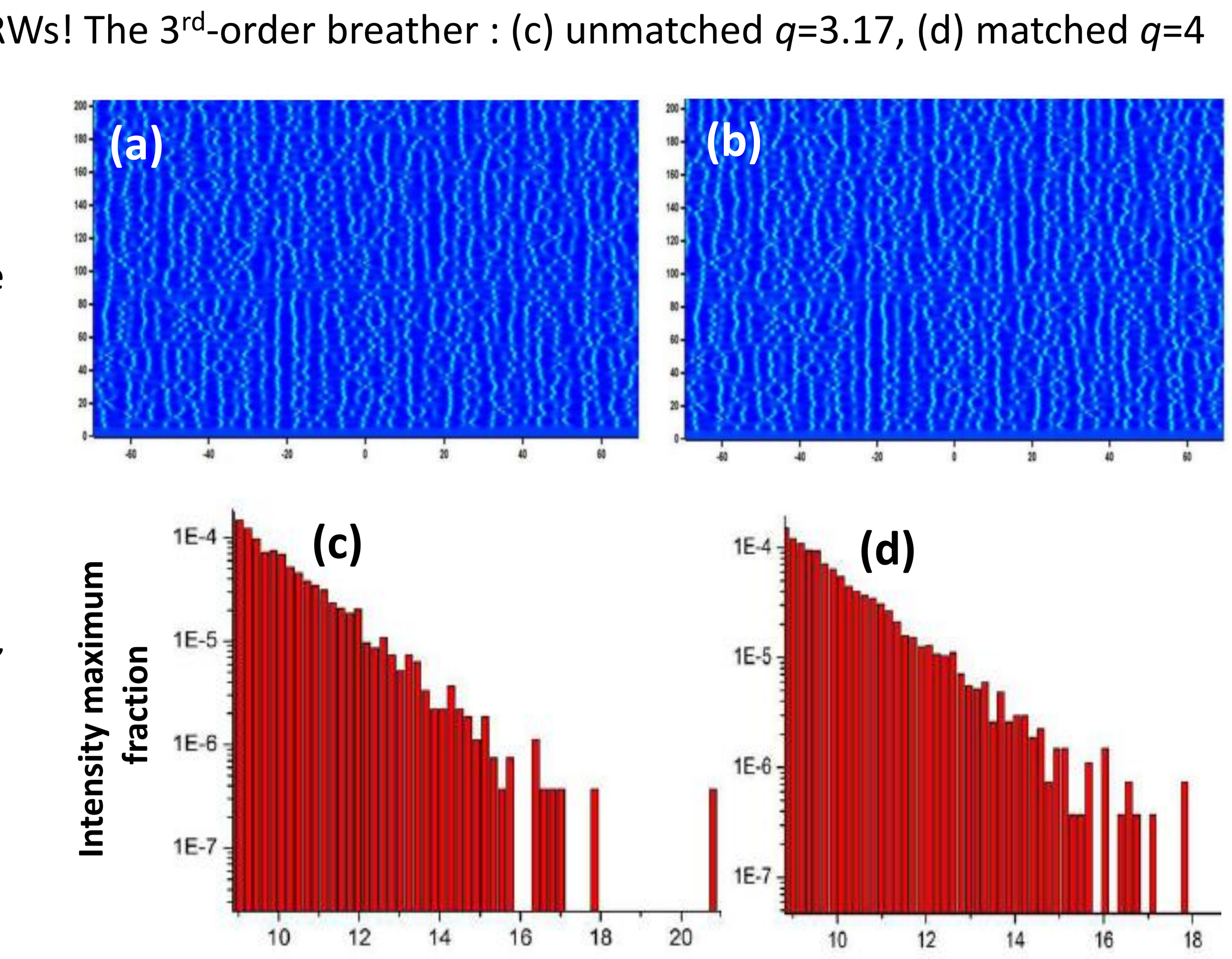

Figure 7: NLSE intensity evolution seeded by white noise (5% amplitude) around the background intensity of 2. (a) Beam propagation method, (b) symplectic algorithm. Statistics of high intensity peaks for (a) and (b) is presented in (c) and (d), respectively.

References:

[1] S. N. Nikolic, O. A. Ashour, N. B. Aleksic, M. R. Belic, S. A. Chin, Nonlinear Dyn. **95**, 2855 (2019).

[2] S. N. Nikolic, O. A. Ashour, N. B. Aleksic, Y. Zhang, M. R. Belic, S. A. Chin, Nonlinear Dyn. **97**, 1215 (2019).

[3] S. Toenger, T. Godin, C. Billet, F. Dias, M. Erkintalo, G. Genty, J. M. Dudley, Sci. Rep. **5**, 10380 (2015).

PHOTONICA 2021 ::: 23 August - 27 August 2021, Belgrade, Serbia